New Phytologist

Exploring *Picea glauca* aquaporins in the context of needle water uptake and xylem refilling

Joan Laur and Uwe G. Hacke

Department of Renewable Resources, University of Alberta, 442 Earth Sciences Building, Edmonton, AB T6G 2E3, Canada

Author for correspondence:
Joan Laur
Tel: +1 780 492 4535
Email: laur@ualberta.ca

Received: *13 January 2014*
Accepted: *9 March 2014*

New Phytologist (2014) **203:** 388–400
doi: 10.1111/nph.12806

Key words: aquaporins, endodermis, foliar water uptake, *Picea glauca*, plasma membrane intrinsic proteins (PIPs), radial water flow, xylem refilling.

Summary

- Conifer needles have been reported to absorb water under certain conditions. Radial water movement across needle tissues is likely influenced by aquaporin (AQP) water channels.
- Foliar water uptake and AQP localization in *Picea glauca* needles were studied using physiological and microscopic methods. AQP expression was measured using quantitative real-time PCR. Members of the *AQP* gene family in spruce were identified using homology search tools.
- Needles of drought-stressed plants absorbed water when exposed to high relative humidity (RH). AQPs were present in the endodermis-like bundle sheath, in phloem cells and in the transfusion parenchyma of needles. Up-regulation of AQPs in high RH coincided with embolism repair in stem xylem. The present study also provides the most comprehensive functional and phylogenetic analysis of spruce AQPs to date. Thirty putative complete AQP sequences were found.
- Our findings are consistent with the hypothesis that AQPs facilitate radial water movement from the needle epidermis towards the vascular tissue. Foliar water uptake may occur in late winter when needles are covered by melting snow and may provide a water source for embolism repair before the beginning of the growing season.

Introduction

Water in xylem is usually thought to move unidirectionally from the soil to the leaves. However, a growing body of evidence indicates that many plants take up water from leaf and/or bark surfaces, and that this can result in reverse water flow in stem xylem (Burgess & Dawson, 2004).

The uptake of intercepted water on leaf surfaces into leaves (foliar uptake) has been demonstrated in plants from a range of dew- and cloud-affected plant communities, including the redwood forest (Burgess & Dawson, 2004; Limm *et al.*, 2009), a mountain pine forest in Tenerife, Spain (Nadezhdina *et al.*, 2010) and tropical cloud forests (Eller *et al.*, 2013; Goldsmith *et al.*, 2013; Gotsch *et al.*, 2014). Dewfall absorption by aerial plant parts has also been reported for the desiccation-tolerant plant *Vellozia flavicans* in the savannas of Brazil (Oliveira *et al.*, 2005).

Many reports of foliar uptake come from studies on conifers. Sparks *et al.* (2001) observed increases in stem water content of *Pinus contorta* during the winter, and offered direct water uptake by stems or foliage as a likely explanation. Water may have originated from melting snow (Sparks *et al.*, 2001). Foliar absorption of intercepted rainfall has been observed in *Juniperus monosperma*, a widely distributed dryland species (Breshears *et al.*, 2008). The conclusion that foliar uptake occurred in this species was based on changes in leaf water potential in response to foliar wetting and the use of isotopically labeled water. Moreover, the response to foliar uptake increased with increasing amounts of plant water stress. Breshears *et al.* (2008) suggested that foliar absorption in *J. monosperma* could play an important role in mitigating water stress and in aiding survival during drought.

Another role for water absorption through the leaves may be to facilitate embolism repair in the xylem of conifers (McCulloh *et al.*, 2011; Mayr *et al.*, 2014) and other plants (Oliveira *et al.*, 2005). If water could be absorbed by leaves, the xylem pressure at the top of tall trees could rise above the pressure predicted on the basis of the height of a tree (McCulloh *et al.*, 2011). Apart from mitigating water stress and potentially facilitating embolism reversal, the reduction in leaf water deficit can also result in improved photosynthesis, stomatal conductance and growth (Boucher *et al.*, 1995; Simonin *et al.*, 2009; Eller *et al.*, 2013). On the basis of all of these findings, it appears that foliar uptake is a relatively widespread and potentially important phenomenon, and that it must be considered in ecophysiological and hydrological models (Breshears *et al.*, 2008; Goldsmith, 2013).

Foliar water uptake may occur when water has coalesced on the leaf surface and the leaf is experiencing a water deficit, that is, when leaves have a more negative water potential than the surrounding atmospheric boundary layer (Goldsmith, 2013). Although more work is required to better understand the anatomical pathways for water entry into the leaf, the available evidence suggests that water is taken up via the cuticle and other leaf

structures (Burkhardt *et al.*, 2012; Eller *et al.*, 2013; North *et al.*, 2013). In leafy twigs of *Picea abies*, water was taken up through the bark (Katz *et al.*, 1989). Fluorescent dye movement suggested that water migrated along the rays and parenchyma cells of the bark and the wood.

In the leaf, water can move through the apoplast or from cell to cell. Where lignified or suberized cell walls are present in the bundle sheath, water must cross cell membranes. Water movement through cell membranes is facilitated and regulated by aquaporins (AQPs). These channel proteins transport water and other molecules, and are found in almost all living organisms. According to Heinen *et al.* (2009), there are three ways by which water exchange across cell membranes is regulated by AQPs: (1) their expression level; (2) their trafficking; and (3) their gating, that is, the opening or closing of channels. Expression is one of the most important methods of AQP regulation, and the study of their expression level and localization is highly relevant to a better understanding of their physiological role (Heinen *et al.*, 2009).

Plant AQPs form a large family of water channel proteins, with 28 members in *Vitis vinifera* (Fouquet *et al.*, 2008), > 30 members in *Arabidopsis* and *Oryza sativa*, and > 50 members in *Populus trichocarpa* (Maurel *et al.*, 2008; Gupta & Sankararamakrishnan, 2009). Plasma membrane intrinsic proteins (PIPs; with two phylogenetic subgroups, PIP1 and PIP2) and tonoplast intrinsic proteins (TIPs) are the most abundant AQPs in the plasma membrane and vacuolar membrane, respectively (Maurel *et al.*, 2008; Gomes *et al.*, 2009). PIPs are thought to represent a major path for cell-to-cell water transport. Their contribution in the cell-to-cell component of root water uptake has been described extensively (Vandeleur *et al.*, 2009; Sakurai-Ishikawa *et al.*, 2011; Laur & Hacke, 2013). Other AQP subfamilies include nodulin-26-like intrinsic membrane proteins (NIPs) and small basic intrinsic proteins (SIPs) (Maurel *et al.*, 2008; Gomes *et al.*, 2009).

The role of AQPs in foliar water uptake has been studied in an epiphytic bromeliad (Ohrui *et al.*, 2007), but little is known about the role of leaf AQPs in the context of foliar uptake in other plant groups. Mayr *et al.* (2014) reported that conifers at the timberline repaired winter embolism in early spring, at a time when the soil was still frozen. Experimental evidence indicated that water (from melting snow) was taken up through needles and/or bark of stems, and that PIPs were present in the needle endodermis during the refilling period in later winter/early spring.

Here, we studied needle water uptake and the role of AQPs in this process under controlled conditions in clonal *Picea glauca* plants. Plants experienced a moderate drought, and were subsequently exposed to high atmospheric humidity without watering the soil. Physiological, anatomical and molecular parameters were monitored during the experiment. We were particularly interested in linking foliar water uptake with embolism repair. The following hypotheses were tested: (1) needles are able to take up water; (2) AQPs in needles are involved in this process; and (3) foliar uptake can play a role in embolism repair.

An important objective related to our second hypothesis was to obtain a better understanding of the tissue-level localization of leaf AQPs, both during drought treatment and after plants had been transferred to a high-humidity environment. The endodermis-like bundle sheath of Pinaceae is positioned between vascular and photosynthetic tissue, and often contains Casparian strips (Liesche *et al.*, 2011). Analogous to the situation in many roots, the endodermis in conifer needles may therefore play an important role in modifying radial water flow. Consistent with this idea and based on the findings of Mayr *et al.* (2014), we expected to find a large amount of AQP protein in the endodermis, particularly after plants experienced conditions conducive to foliar water uptake.

Although much has been learned about AQP expression and function in a variety of model plants, very little is known about AQPs in conifers, including spruce. To our knowledge, the AQP family in spruce has not been characterized, although the expression pattern of a few AQP homologs has been investigated in the seedlings, mature roots and needles of *P. abies* (Oliviusson *et al.*, 2001; Hakman & Oliviusson, 2002). Therefore, a first step in this study was to comprehensively analyze expressed members of the spruce AQP family in order to identify candidate genes involved in the foliar uptake of water.

Materials and Methods

Plant material and growing conditions

Three-year-old white spruce plants (*Picea glauca* (Moench) Voss, clone EPB-3858) were obtained from the Saint-Modeste Nursery (QC, Canada). Plants were established for 2 months in 3.8-l containers with Sunshine Mix #4 (Sun Gro Horticulture Canada Ltd, Seba Beach, AB, Canada) under the following conditions: 16 h : 8 h day : night cycle, 24°C : 20°C day : night temperature, *c.* 50% daytime relative humidity (RH) and photosynthetically active radiation of 350 $\mu mol\ m^{-2}\ s^{-1}$ at plant level. Plants were watered twice a week and fertilized on a weekly basis with 200 ml of 20 : 20 : 20 N : P : K fertilizer applied at 0.5 $g\ l^{-1}$. One group of plants was well watered (control group); another group of plants was subjected to a drought stress treatment, where water was withheld until the stem water potential (Ψ_{Stem}) was near −3 MPa. This target water potential was associated with *c.* 20% loss of hydraulic conductivity according to the vulnerability curve (for details, see later). To study the ability of shoots to absorb water and to repair xylem embolism after drought treatment, a subset of drought-stressed plants was placed in a humidified box (*c.* 100% RH; high-humidity plants). Pots were completely sealed with plastic bags, using tape and parafilm, to prevent water from reaching the soil. The volumetric soil water content was measured using an EC-5 sensor (Decagon Devices, Pullman, WA, USA). The measurements described below were carried out 2, 26 and 50 h after plants had been placed in the high-humidity box (exposure to high humidity started at 09:00 h). Another subset of drought-stressed plants was rewatered; these plants were not transferred to the high-humidity environment.

Relative water content (RWC)

To evaluate the effects of foliar water absorption on the water relations of needles and twigs, we determined the RWC of

needles (five needles per plant) and twigs (one twig per plant) from six individual plants. The RWC was calculated as (fresh weight – dry weight)/(turgid weight – dry weight). To determine turgid weight, needles and twigs were floated on distilled water for 48 h. Dry weight was determined after drying samples at 70°C for 48 h. RWC measurements were made before (control) and after (dehydrated) overnight drying on the bench top. Bench-dried samples were then transferred to a high-humidity environment (*c.* 100% RH) for 16 h (high RH). To prevent water uptake through the part of the needle base, this surface was covered with mineral oil. To assess the role of needles in shoot water uptake, we also measured the RWC of the leaf-less basal part of twigs in control, dehydrated and high-RH conditions. The cut ends of these 3–5-cm-long basal twig segments were covered with parafilm before exposure to high RH.

Needle anatomy

An effort was made to study the anatomy and chemical composition of needle tissue, as well as possible hydrophilic pathways in needles. Alcian blue (0.5% w/v) was used to stain mucilage, which generally has a high water-binding capacity because of the high concentration of hydroxyl groups (Clifford *et al.*, 2002). Hand-cut needle cross-sections were observed using a light microscope (DM3000; Leica, Wetzlar, Germany) and a digital camera (DFC420C; Leica). Fresh tissue was fixed in FAA (10% formaldehyde, 5% acetic acid, 50% ethanol) under vacuum for 1 h, stored in FAA for 16 h at 4°C and embedded in paraffin as described previously (Almeida-Rodriguez *et al.*, 2011). The periodic acid-Schiff reaction was also used to identify hydrophilic polysaccharide compounds, such as mucilage, glycolipids and glycoproteins (Eller *et al.*, 2013). For the detection of lignin, needle cross-sections were stained with 1% (w/v) phloroglucinol in 35% (v/v) HCl. Photographs were taken within 30 min of phloroglucinol–HCl staining.

Water potential and stomatal conductance

Water potential was measured after shoots had been sealed in aluminum foil and plastic bags the day before harvesting to ensure water potential equilibration (Begg & Turner, 1970). Stem water potential (Ψ_{Stem}) was measured using a pressure chamber (Model 1000; PMS Instruments, Albany, OR, USA). Stomatal conductance was measured with a steady state porometer (LI-1600; Li-Cor, Lincoln, NE, USA) on at least five plants per group, and normalized by needle surface area (Sigma Scan 5.0; Jandel Scientific, San Rafael, CA, USA).

Hydraulic measurements

The percentage loss of hydraulic conductivity (PLC) was measured using a conductivity apparatus (Sperry *et al.*, 1988), as described previously (Plavcová & Hacke, 2012). Segments corresponding to the previous year of growth (2012) were used for hydraulic measurements. Segments were gradually trimmed under water to a final length of 14.2 cm. A vulnerability curve was generated using the centrifuge method, as described previously (Schoonmaker *et al.*, 2010). Curves were fitted with a Weibull function.

Analysis of spruce AQP sequences

Sequence information from the *P. glauca* expressed sequence tag (EST) database of the National Center for Biotechnology Information (NCBI) (http://www.ncbi.nlm.nih.gov/) was used for BLASTn and tBLASTn homology searches (Altschul *et al.*, 1997). The sequences of *Arabidopsis thaliana* (Johanson *et al.*, 2001), *Zea mays* (Chaumont *et al.*, 2001) and *Physcomitrella patens* (Danielson & Johanson, 2008) were used as queries. Bioinformatics analyses were conducted using the Mobyle web platform (Néron *et al.*, 2009). EST sequence assembly was performed with CAP3 (Huang & Madan, 1999). The concordance of this *de novo* assembly with a previously published *P. glauca* gene catalog (Rigault *et al.*, 2011) was assessed manually.

The recent publication of the *Picea* sp. draft genome (Birol *et al.*, 2013; Nystedt *et al.*, 2013) allowed us to assess intron positions; when discovered in the *P. abies* 1.0 database, complete coding sequences were included for further analysis (Supporting Information Table S1). All accession numbers are given in Table 1. The alignment of the deduced amino acid sequences (sixpack EMBOSS module; Rice *et al.*, 2000) was generated and edited with Clustal Omega 1.1.0 (Sievers *et al.*, 2011). The quality of the alignment was assessed by its norMD score (Thompson *et al.*, 2001) (Fig. S1, Notes S1). Maximum-likelihood, neighbor-joining and unweighted pair group method with arithmetic average (UPGMA) techniques were used to perform phylogenetic analyses employing a bootstrapping procedure (1000 bootstraps). The resulting trees, including 30 complete AQP sequences, were displayed using the Figtree program (http://tree.bio.ed.ac.uk/software/figtree) (Figs S2, S3, Notes S1). Transmembrane regions were detected using TopPred II 0.01 (Claros & von Heijne, 1994). Aromatic/arginine (Ar/R) selectivity filters were identified by manual inspection. Subcellular localizations were predicted using Plant-mPLoc (Chou & Shen, 2010) and WoLF PSORT (Horton *et al.*, 2007). The expression profile of each AQP gene was estimated by tallying the tissue distribution of clustering ESTs in non-normalized libraries (Alba *et al.*, 2004) and using IDEG6 (Romualdi *et al.*, 2003).

Gene transcript measurements by quantitative real-time PCR

Needles were collected, immediately frozen in liquid nitrogen and stored at −80°C until analysis. Samples were always collected at the same time of day to minimize any diurnal effect on AQP expression. Total RNA was extracted from needles of three to four plants per treatment following the cetyltrimethylammonium bromide (CTAB) method of Chang *et al.* (1993) modified by Pavy *et al.* (2008). RNA quality was assessed on an agarose gel and quantified with a spectrophotometer (Nanodrop ND-1000; Thermo Scientific, Wilmington, DE, USA). One microgram of total RNA was treated with deoxyribonuclease I (Invitrogen, Carlsbad, CA, USA) and used as template for first-strand cDNA

Table 1 Features of spruce (*Picea glauca*) major intrinsic proteins (MIPs)

	cDNA clone accession	Amino acids	Number of clones	TMHs	Tissue specificity[1]	Subcellular location	NPA motifs	Ar/R filters
PgPIP1;1	GQ03401_M18	292	52	6	R N S C	PM	NPA/NPA	F H T R
PgPIP1;2	GQ03610_A06	288	79	6	R N S C	PM	NPA/NPA	F H T R
PgPIP1;3	GQ02828_J14	285	31	6	S N	PM	NPA/NPA	F H T R
PgPIP2;1	GQ03111_E12	282	26	6	R N S C	PM	NPA/NPA	F H T R
PgPIP2;2	GQ02901_B20	282	71	6	R N S C	PM	NPA/NPA	F H T R
PgPIP2;3	GQ03703_H07	282	3	6	R S	PM	NPA/NPA	F H T R
PgPIP2;4	GQ0132_J09	282	5	6	R	PM	NPA/NPA	F H T R
PgPIP2;5	GQ03124_N20	269	5	6	C	PM	NPA/NPA	F H T R
PgPIP2;6	GQ03705_D15	284	49	6	R N S	PM	NPA/NPA	F H T R
PgPIP2;7	GQ02905_E13	282	77	6	R S C	PM	NPA/NPA	F H T R
PgPIP2;8	GQ02902_L14	280	16	6	R N S	PM	NPA/NPA	F H T R
PgPIP2;9	GQ03002_G07	280	6	6	S	PM	NPA/NPA	F H T R
PgPIP2;10	GQ03011_G23	275	15	6	R S	T-PM	NPA/NPA	F Y T R
PgPIP2;11	GQ03010_E09	275	10	6	S	T-PM	NPA/NPA	F Y T R
PgPIP2;12	GQ03001_P18	283	57	6	R S	T-PM	NPA/NPA	F H T R
PgPIP2;13	GQ03216_M18	272	22	6	S	PM	NPA/NPA	F H T R
PgTIP1;1	GQ0197_E19	253	5	6	R	T	NPA/NPA	H I A R
PgTIP1;2	GQ03116_D08	253	12	6	R	C-T	NPA/NPA	H I A R
PgTIP1;3	GQ02908_P24	253	11	6	S	C-T	NPA/NPA	H I A R
PgTIP1;4	GQ03501_N03	255	18	6	R N S	C-T	NPA/NPA	H I A R
PgTIP1;5	GQ0206_N10	253	56	6	R S	T	NPA/NPA	H I A R
PgTIP2;1	GQ03915_M04	250	199	6	R N S C	PM-T	NPA/NPA	H I G R
PgTIP2;2	WS0323_F18	211	3	5	S	T	NPA/NPA	H I G R
PgTIP4;1	GQ0201_M19	248	9	6–7	R S	T	NPA/NPA	H I A R
PgTIP4;2	GQ04012_G01	250	1	6–7	S	T	NPA/NPA	H I A R
	WS02617_N14	115	1	3		T	NPA/NPA	- - A R
PgNIP1;1	GQ03122_A02	280	12	6	S	PM	NPA/NPA	WV AR
	GQ03202_N13	195	2	4	S	PM	NPA/NPA	- V A R
PgNIP2;1	GQ03207_J07	296	6	6	N S	PM	NPA/NPA	A I G R
	GQ03237_P23	42	1	0	S	na	–	–
PgNIP3;1	GQ03810_B10	294	13	6	S	T-PM	NPA/NPA	A I A R
PgNIP3;2	GQ03701_J12	215	1	6	S	PM	NPA/NPA	A I G R
PgSIP1;1	GQ03414_P10	238	29	6	R N S C	T	NPT/NPA	L T P N
	GQ04011_K04	138	4	2	S R	PM-T	NPV/NPA	- K P T

Gene names, accession number, length of deduced polypeptides, number of cDNA clones included in the assembly, predicted number of transmembrane helix domains (TMHs), tissue specificity of expressed sequence tags (ESTs), predicted subcellular location (C, cytoplasm; PM, plasma membrane; T, tonoplast; na, not available) and conserved residues (NPA motifs, Ar/R filters) are summarized.
[1]Tissues used for cDNA library preparation are listed: C, reproductive parts; N, needles; R, roots; S, stems. Bold gene names indicate the candidate genes presented in this study.

synthesis with SuperScript II and random nucleotide primers (Invitrogen) following the manufacturer's instructions. cDNA quality was checked by PCR with intron-spanning actin primers. Putative needle-expressed PIP genes were selected (Table 1). Specific primers (Table S2a) were designed according to Rutledge & Stewart (2010) using the QuantPrime online tool (Arvidsson *et al.*, 2008). PCR efficiency (E) was determined from a five-point cDNA serial dilution, according to: $E = 10[-1/\text{slope}]$. All selected primer pairs showed correlation coefficients of $R^2 > 0.98$ and primer efficiency values ranging between 1.97 and 2.07. Quantitative real-time PCR was performed on a 7900 HT Fast Real-Time PCR system (Applied Biosystems, Foster City, CA, USA) as described previously (Laur & Hacke, 2013).

Gene transcript localization by *in situ* hybridization

In situ hybridization was performed as described previously (Karlgren *et al.*, 2009), with the following adjustments: protease K digestion was shortened to 10 min at room temperature (1 ng ml^{-1}), and a carbethoxylation reaction (0.1% diethylpyrocarbonate (DEPC) in phosphate-buffered saline (PBS), 15 min) was included during pre-hybridization (Braissant & Wahli, 1998). Primers were designed (Table S2b) using the QuantPrime online tool. PCR amplicons were ligated (pCRII vector TOPO cloning kit; Invitrogen) and sequenced to determine orientation. Riboprobes were generated by *in vitro* transcription and labeled with digoxigenin (DIG) using Sp6 and T7 RNA polymerase with the DIG RNA labeling kit (Roche Applied Science, Indianapolis, IN, USA) after 5′-overhang linearization of the plasmid with *Eco*RV and *Bam*HI restriction enzymes, respectively (Invitrogen). To ensure high specificity and to avoid cross-hybridization between gene family members, the hydrolysis step was not performed as the probes were *c.* 300 bp long. Slides were mounted with a synthetic resin (Permount; Fisher Scientific, Ottawa, ON, Canada). Images were taken using a light microscope as already described.

Immunolocalization

Samples were fixed in FAA medium under vacuum for 1 h and stored in FAA for 16 h at 4°C. Next, samples were embedded, sectioned, dewaxed and rehydrated as described previously (Almeida-Rodriguez *et al.*, 2011). Before the first immunoreaction, cross-sections were incubated for 45 min with blocking solution (BS; 1.5% (w/v) glycine, 5% (w/v) bovine serum albumin, 0.1% (v/v) Tween-20 in PBS) following the protocol of Gong *et al.* (2006). Primary antibodies against the 42 N-terminal amino acids of AtPIP1;3 (Kammerloher *et al.*, 1994) and the conserved 10 amino acids of the C-terminus of PIP2 AQPs (similar to Daniels *et al.*, 1994) were included (see alignment in Fig. S4). Secondary antibodies were pre-absorbed with plant tissue extract. DyLight 549-conjugated rabbit anti-chicken secondary antibody (Fisher Scientific, Hampton, NH, USA) and HiLyte Fluor 555-conjugated rabbit anti-mouse secondary antibody (AnaSpec Inc., Fremont, CA, USA) were applied for 2 h at 37°C. Slides were mounted with Permount. Images were taken with a Zeiss LSM 700 confocal microscope (Carl Zeiss, Oberkochen, Germany).

Statistical analysis

All statistical analyses were carried out using SigmaPlot 11.0 (Systat, Point Richmond, CA, USA). Differences caused by the effect of treatments and growing conditions were analyzed using a one-way ANOVA followed by a Tukey's test. For all tests, differences were considered to be significant at $P \leq 0.05$.

Results

Needle water uptake and anatomy

We first asked whether foliar uptake occurred in *P. glauca*, and whether it had a significant impact on needle water status. The RWC of needles of well-watered control plants was 94.5%; bench-dried needles had an RWC of 65.5% (Table 2). After needles had been exposed to high humidity for 16 h, their RWC recovered to an intermediate level, indicating that water uptake occurred.

RWC measurements were also performed on twigs. After bench drying, the RWC of twigs dropped significantly, but recovered to control levels after twigs had been exposed to high humidity (Table 2). By contrast, a significant recovery of RWC did not occur when needles were detached from twigs after bench drying, indicating that water uptake was facilitated by needles.

To study the potential anatomical pathways for water uptake, needle sections were prepared for light microscopy and stained. Alcian blue staining indicated that stomata were associated with mucilage (Fig. 1a), which generally comprised a mixture of polysaccharides. A high concentration of hydrophilic carbohydrates was detected in the epidermis, hypodermis and other cell types (Fig. 1b), which may have facilitated water retention within the tissues. Phloroglucinol–HCl staining revealed the presence of lignified cell walls in bundle sheath cells (especially in radial cell walls), transfusion tracheids and xylem tracheids (Fig. 1c).

Table 2 Relative water content (RWC) of white spruce (*Picea glauca*) needles

Experimental treatment	Needle RWC[1] (%)	Twig RWC[2] (%)
Control	94.49 (2.60)^{A}	81.31 (1.19)^{A}
Dehydrated	65.47 (1.44)^{B}	73.40 (0.96)^{B}
High RH	78.39 (2.23)^{C}	82.27 (2.47)^{A}
High RH, no needles	na	77.28 (1.60)^{AB}

[1]RWC of needles was measured before (control) and after (dehydrated) overnight drying on the bench top. Bench-dried needles were then transferred to a high-humidity environment (*c.* 100% RH) for 16 h (high RH). na, not applicable.
[2]RWC of twigs subjected to the same experimental treatment as needles. To assess the importance of foliage on the water absorption of twigs, basal leaf-less segments of dried twigs were exposed to high RH for 16 h (high RH, no needles). The standard error of the mean is given in parentheses. Different letters indicate significant differences between treatments ($n = 6$; $P \leq 0.05$).

Distribution of PIP1 and PIP2 AQPs in needle cross-sections

To test the hypothesis that AQPs in needles are involved in foliar uptake, we first examined the detailed localization of PIP1 and PIP2 using confocal fluorescence microscopy (Fig. 2). In well-watered plants, PIP1s were present in the endodermis and in phloem (Fig. 2a). Needle cross-sections of drought-stressed plants exhibited minimal labeling (Fig. 2b). Controls with no primary antibody showed a very weak or no background signal (Fig. 2c).

Needle sections taken as early as 2 h after the increase in RH exhibited strong immunolabeling of the endodermis (Fig. 2d). The labeling intensity for PIP1 in endodermis, phloem and transfusion parenchyma cells peaked after 8 h of exposure to high humidity (Fig. 2e). After 26 h at high humidity, PIP1 labeling was still evident in the endodermis, but the intensity of the signal in phloem and transfusion parenchyma was reduced (Fig. 2f).

A similar trend was observed for PIP2 (Fig. 2g–l), although the distribution of PIP1 and PIP2 showed some interesting differences. Under conditions that would be conducive to foliar water uptake (i.e. exposure to high humidity after a drought treatment), PIP1 labeling was more focused than PIP2 labeling in the endodermis, suggesting that PIP1s are involved in the regulation of water movement across the bundle sheath.

PIP2s appeared to be more widely distributed than PIP1s within the central cylinder. Although some PIP2 labeling was detected in the endodermis, strong signals were also apparent in the plasma membrane of transfusion parenchyma cells (asterisks in Fig. 2j–l) and in the phloem, including in cells that appeared to be Strasburger cells (arrowheads in Fig. 2j,k). Intense plasmodesmatal contact exists between sieve cells and Strasburger cells, and Strasburger cells are regarded as companion cell equivalents (Sauter *et al.*, 1976). Labeling also occurred in the mesophyll. PIP2s may therefore facilitate water transport between most, if not all, living cells in the central cylinder and mesophyll.

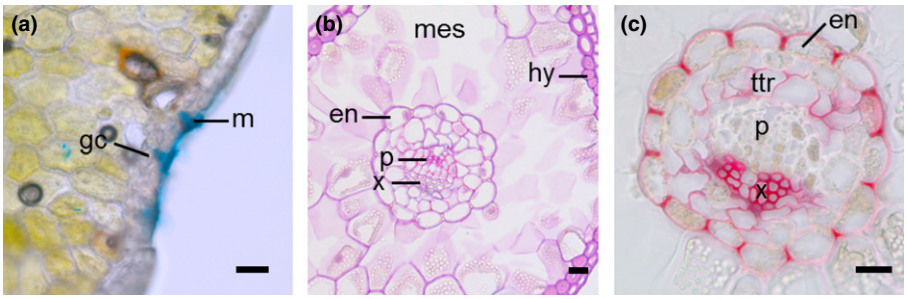

Fig. 1 Light microscopy images of *Picea glauca* needle cross-sections. (a) Section showing a stoma (gc, guard cells) covered by mucilage (m). The section was stained with Alcian blue. (b) A cross-section in which polysaccharides were stained with periodic acid-Schiff reagent. A high polysaccharide content (stained pink) was detected in the cell walls of the epidermis, hypodermis (hy), endodermis (en) and phloem (p) cells. mes, mesophyll; x, xylem. (c) Cross-section stained with phloroglucinol–HCl; lignified cell walls are shown in red. Lignin was detected in radial cell walls of the endodermis, in transfusion tracheids (ttr) and in xylem tracheids. Bars, 20 μm.

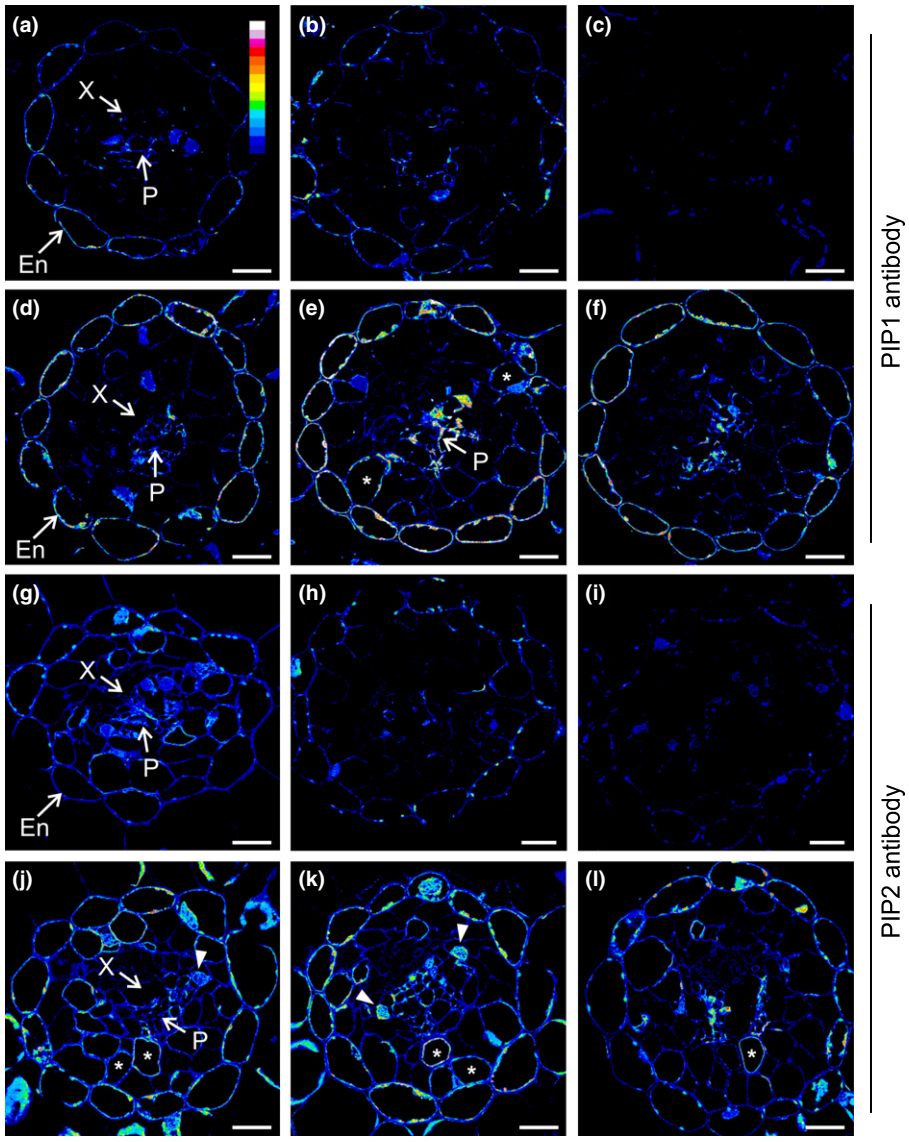

Fig. 2 Confocal laser scanning micrographs showing the localization of aquaporin proteins in *Picea glauca* needle cross-sections. Images were taken at an identical setting and were color-coded with an intensity look-up-table (LUT; displayed in a), in which black was used to encode background, and blue, green, yellow, red and white to encode increasing signal intensities. (a–f) PIP1 localization in needles; (g–l) PIP2 localization in needles. Cross-sections of well-watered (a, g) and drought-stressed (b, h) plants. (c, i) Controls with no primary antibody indicate minimal background fluorescence. Sections of previously drought-stressed plants were taken 2 h (d, j), 8 h (e, k) and 26 h (f, l) after plants had been transferred to a high-humidity environment. PIP1 labeling was strongest in the endodermis (En) and in phloem (P). Strong PIP2 signals were detected in the phloem (putative Strasburger cells labeled by arrowheads in j and k) and in transfusion parenchyma (asterisks in j–l). No signal was detected in the xylem (X). Bars, 20 μm.

Spruce AQP family

As a first step in investigating the expression and function of individual AQP genes in spruce, we identified expressed members of the spruce AQP gene family. Information, including gene names, accession numbers, length of the deduced polypeptides and predicted subcellular location, is given in Table 1. A total of 1188 ESTs corresponding to putative major intrinsic proteins (MIPs)

was identified in the NCBI database (http://www.ncbi.nlm.nih.gov/). Based on sequence overlap, a non-redundant set of 34 contigs was retrieved from the EST assembly (Table 1). The 30 putative complete MIP sequences could be grouped into PIP, TIP, NIP and SIP subfamilies (Figs 3, S1–S3, Notes S1).

We also took advantage of the recent sequencing of the *Picea* sp. genome to complete our investigation. Searches of the *P. abies* 1.0 draft genome at ConGenIE, using the complete set of retrieved *P. glauca* AQPs, as well as PpXIPs, PtXIPs, PpGIP1;1 and PpHIP1;1 protein sequences, resulted in the identification of 30 complete homolog sequences for *P. abies* (for the phylogenetic relations of all *Picea* AQP members, see Figs 3, S2, S3, Table S1, Notes S1). Sequences corresponding to the X intrinsic protein (XIP), GlpF-like intrinsic protein (GIP) and hybrid intrinsic protein (HIP) subfamilies were not retrieved in either *P. abies* or *P. glauca* genomic databases.

Compilation of these data allowed us to systematically name PgAQPs (Tables 1, S1, Figs 3, S1–S3, Notes S1). In total, 16 PgPIPs, nine PgTIPs, four PgNIPs and one PgSIP full-length sequences were identified from transcriptomic data. PIP subfamily members were further divided into two subgroups with three PIP1s and 13 PIP2s. All PIP genes shared common sequence features (NPA boxes, Ar/R residues), except for PIP2;10 and PIP2;11, where histidine (H) was substituted by tyrosine (Y), indicating a possible difference in substrate specificity (Table 1, Fig. S1). All of the PIP sequences were predicted to localize to the plasma membrane (Table 1).

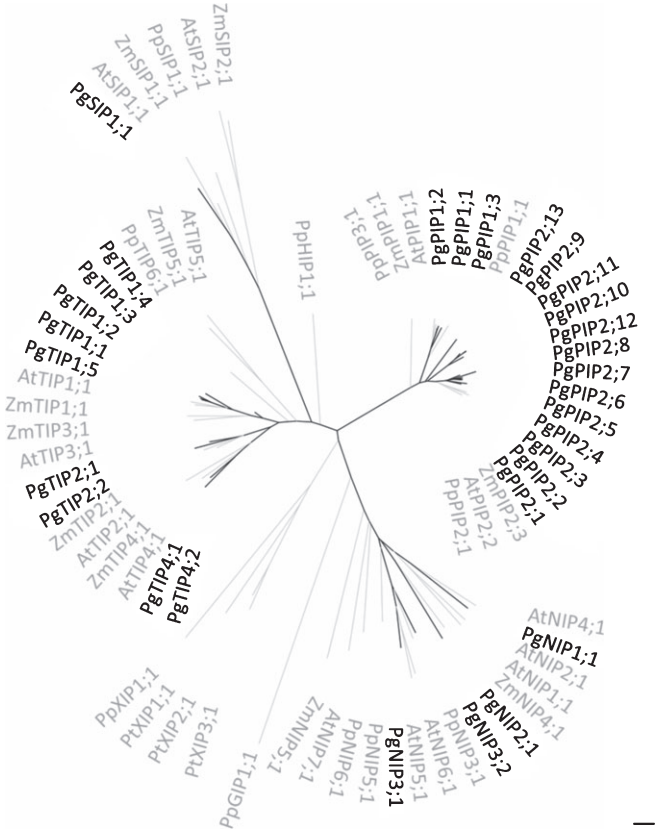

Fig. 3 Phylogenetic analysis of 30 aquaporins (AQPs) expressed in *Picea glauca*. The phylogeny was inferred using maximum likelihood. *Picea glauca* AQPs (PgAQPs) are shown in black type; AQPs from *Zea mays* (ZmAQPs), *Arabidopsis thaliana* (AtAQPs) and *Physcomitrella patens* (PpAQPs) are represented by gray type. In *P. glauca*, four subfamilies can be identified (plasma membrane intrinsic proteins (PIPs), tonoplast intrinsic proteins (TIPs), nodulin-26-like intrinsic membrane proteins (NIPs) and small basic intrinsic proteins (SIPs)). Also note the close relationship between PIP subfamily members. The bar indicates the mean distance of 0.1 changes per amino acid residue.

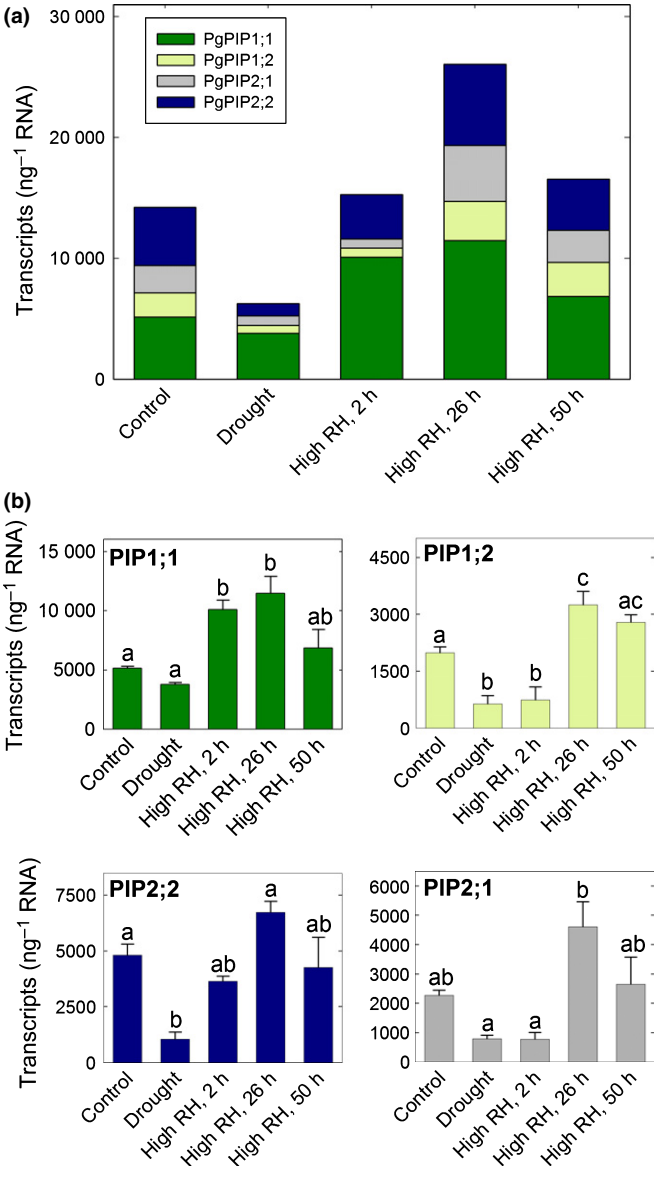

Fig. 4 Aquaporin transcript amounts in needles of well-watered (Control) and drought-stressed (Drought) white spruce (*Picea glauca*) plants. Transcript amounts were also measured 2, 26 and 50 h after drought-stressed plants had been transferred to a high-humidity environment. (a) Cumulative aquaporin transcript amounts in needles. Individual genes are labeled with different colors. Among the different transcripts, *PgPIP1;1* ranked first in terms of its proportion to the total number of mRNA molecules. (b) Transcript abundance of *PgPIP1;1*, *PgPIP1;2*, *PgPIP2;1* and *PgPIP2;2*. Values are means ± SE from three biological samples which were tested in triplicate. Significant differences are indicated by unique letters ($P \leq 0.05$).

Expression of selected AQP genes in needles

The tissue specificity for each of the *P. glauca* AQPs was studied using the EST database. The available 28 EST libraries are an unbiased representation of the tissue-specific transcriptome. Two PIP1 (*PgPIP1;1*, *PgPIP1;2*) and two PIP2 (*PgPIP2;1*, *PgPIP2;2*) candidate genes that have been reported to be expressed in needles were selected for analysis.

All of the four genes showed significant changes in expression during the treatments (Fig. 4). Of the genes studied here, *PgPIP1;1* and *PgPIP2;2* ranked first in terms of their proportion to the total number of mRNA molecules (Fig. 4a, dark green and dark blue portions of the bars). The drought treatment resulted in more than a two-fold reduction in the cumulative transcript amount relative to well-watered control plants (Fig. 4a). This was mainly driven by reduced expression levels of *PgPIP1;2*, *PgPIP2;2* and *PgPIP2;1* (Fig. 4b). Transcript levels increased rapidly after plants were exposed to high RH. After only 2 h, the cumulative number of AQP mRNA molecules was equivalent to the level found in well-watered control plants, and peaked 26 h after the transfer to high humidity. All four genes contributed to this peak in transcript levels after 26 h.

An analysis of the expression patterns of individual genes (Fig. 4b) revealed that there were two types of response. Up-regulation of *PgPIP1;1* and *PgPIP2;2* was detected as soon as 2 h after exposure to high humidity. By contrast, expression levels of *PgPIP1;2* and *PgPIP2;1* remained low 2 h after transfer to high humidity, but increased by more than five-fold (relative to drought levels) 26 h after transfer to high humidity.

Tissue localization of expression

In situ hybridization experiments revealed interesting tissue distribution patterns of expression. *PgPIP1;1* and *PgPIP2;2*, which showed the highest transcript levels among the four genes studied (Fig. 4), were expressed in phloem and in transfusion parenchyma cells (Fig. 5e,f). In contrast with *PgPIP2;2*, expression of *PgPIP1;1* was also prominent in endodermis cells. The *PgPIP1;2* signal was constrained to phloem cells (Fig. 5g). This specific expression pattern is consistent with the relatively low transcript level of this particular gene (Fig. 4). Expression of *PgPIP2;1* was evident in individual phloem cells and in transfusion parenchyma, but not in the endodermis (Fig. 5h).

Linking foliar uptake with embolism repair in stems

To test whether foliar uptake can play a role in embolism repair, we measured physiological parameters in plants before and during drought treatment, as well as after plants had been moved to a high-humidity environment. Well-watered control plants had a Ψ_{Stem} value of -0.6 ± 0.1 MPa ($\pm$ SE, $n \geq 5$), which was associated with minimal xylem embolism in stems (Fig. 6). The drought treatment resulted in a decrease in Ψ_{Stem} to -2.9 ± 0.1 MPa and a $16.1 \pm 1.8\%$ loss of hydraulic conductivity. Consistent with a relatively steep increase in embolism levels at xylem pressures more negative than -2 MPa (Fig. 7), the drought treatment was associated with stomatal closure (Fig. 6b).

Figure 7 shows a more detailed picture of the refilling dynamics of individual plants; each data point represents an individual plant. The amount of xylem embolism measured in drought-stressed plants (Fig. 7, red circles) agreed with predictions derived from the centrifuge-generated vulnerability curve measured on similar plant material. The vulnerability curve indicated that stems experienced a 50% loss of hydraulic conductivity (P50) at a xylem pressure of -4.2 MPa (Fig. 7, inset). Plants that were rewatered after the drought treatment showed partial or complete recovery from xylem embolism within 2 and 8 h, respectively (Fig. 7, gray symbols). Plants that were transferred to the high-humidity environment had not repaired embolism after 8 h (Fig. 7, HH 8 h), but exhibited refilling after 26 and 50 h (Fig. 7, HH 26 and 50 h), although xylem pressures were still substantially negative (-2.4 ± 0.1 and -2.1 ± 0.1 MPa, respectively).

Discussion

The present study was conducted to gain a better understanding of foliar water uptake in *P. glauca*, a common species in the boreal forest of North America. We explored the potential role of

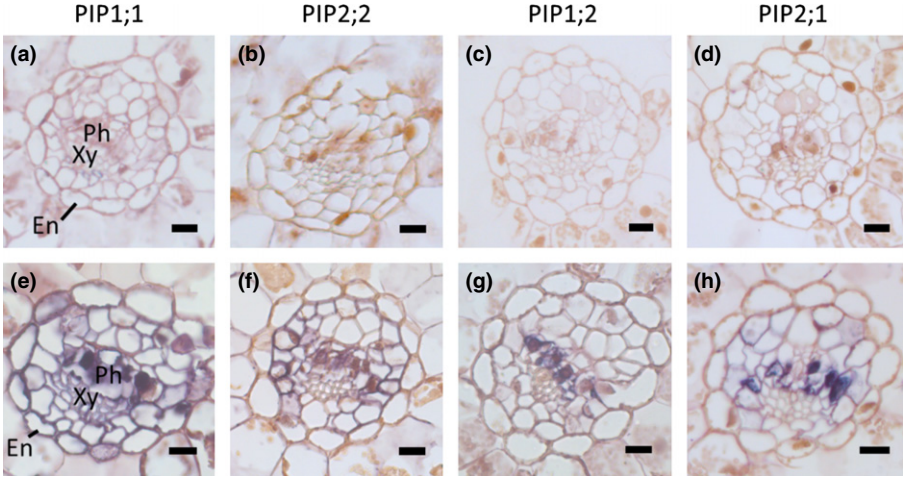

Fig. 5 *In situ* mRNA hybridization of four aquaporin genes in needle cross-sections of *Picea glauca*. (a–d) Negative controls hybridized with digoxigenin (DIG)-labeled sense probes. Sections in (e–h) were hybridized with DIG-labeled antisense *PgPIP1;1* (e), *PgPIP2;2* (f), *PgPIP1;2* (g) and *PgPIP2;1* (h) RNA probes. Regions of aquaporin expression are indicated by dark purple staining. *PgPIP1;1* and *PgPIP2;2* exhibited high expression in the vascular cylinder and in endodermis cells (En). Ph, phloem; Xy, xylem. Bars, 25 μm.

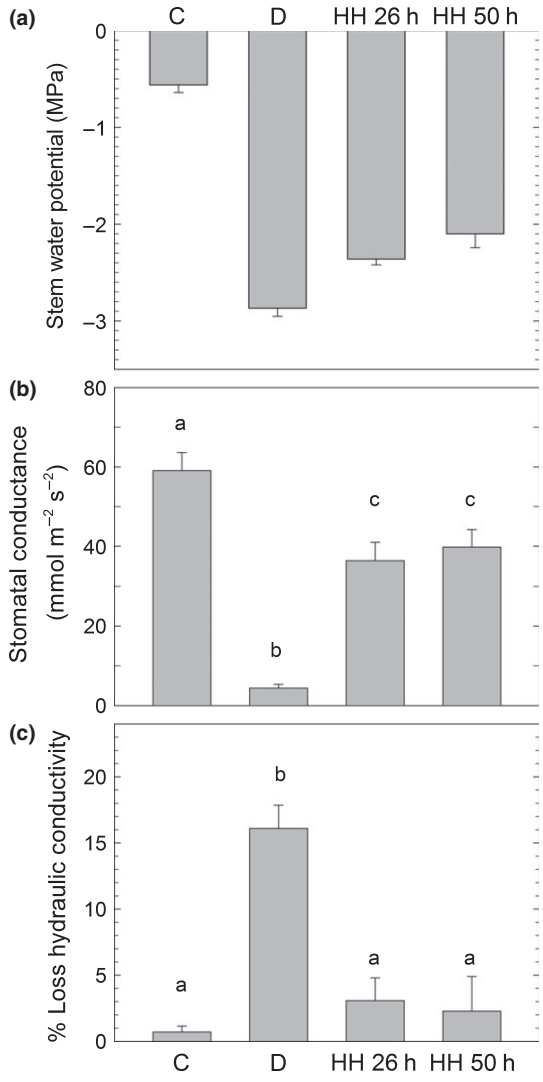

Fig. 6 Stem water potential (a), stomatal conductance (b) and xylem embolism (expressed as percentage loss of hydraulic conductivity) (c) in white spruce (*Picea glauca*) saplings. Plants were grown under well-watered (C) or drought (D) conditions. After drought treatment, plants were kept in a high-humidity environment (without watering the pots) for 26 h (HH 26 h) and 50 h (HH 50 h). Values are means ± SE ($n \geq 5$). Significant differences are indicated by unique letters.

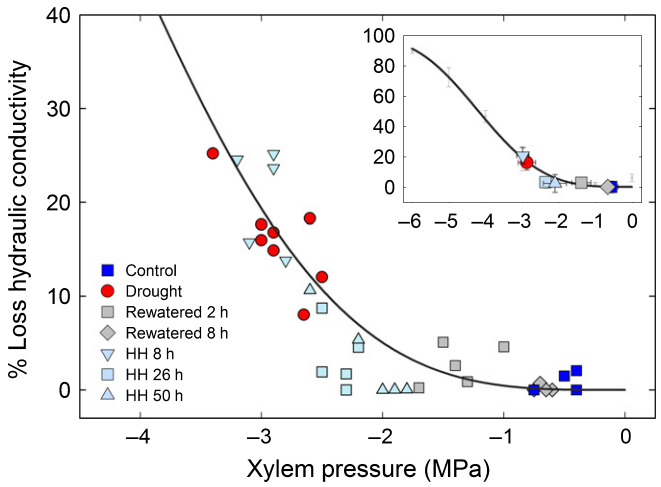

Fig. 7 Effect of a change in water availability on xylem embolism in white spruce (*Picea glauca*) saplings. Vulnerability curve (solid line) and native values of percentage loss of conductivity plotted against the native xylem pressure for stem segments of plants grown under well-watered (Control) or drought (Drought) conditions. Xylem embolism and xylem pressure were also measured in drought-stressed plants 2 and 8 h after rewatering, and in previously drought-stressed plants that were exposed to a high-humidity environment for 8 h (HH 8 h), 26 h (HH 26 h) and 50 h (HH 50 h). An overview of the complete vulnerability curve and native values of xylem embolism plotted against the native xylem pressure for each group (mean ± SE; $n \geq 5$) is shown in the upper right corner of the figure.

AQPs in foliar uptake, and impacts on xylem refilling. The remarkably complex anatomy of conifer needles (Fig. 1; Liesche *et al.*, 2011) and the numerous well-documented cases of needle water uptake (Burgess & Dawson, 2004; Breshears *et al.*, 2008; Limm *et al.*, 2009) make conifer needles an interesting model for the investigation of foliar uptake and potential implications for xylem refilling.

Based on the observed increases in RWC in plants exposed to high humidity, we conclude that drought-stressed needles of *P. glauca* are capable of absorbing water. The occurrence of mucilage and the presence of hydrophilic carbohydrates in the epidermis and hypodermis may facilitate water uptake and water retention by needles. Stomata were at least partially opened at high humidity (Fig. 6b), and so water uptake via stomata would seem possible (Burkhardt, 2010). Foliar water uptake and subsequent refilling also occurred in timberline trees in late winter when the soil was still frozen and when trees were still disconnected from soil water (Mayr *et al.*, 2014).

Depending on the water potential gradients, water may refill the plant from two directions (Goldsmith, 2013; his fig. 1b). Our experiment was designed to restrict water uptake to aboveground plant parts. During drought treatment, water was withheld for many days, and so there was sufficient time for soil and plant water potentials to equilibrate. Before the transition to high RH, pots were carefully covered. The soil water content of high-humidity plants remained at the same low level as seen in drought-stressed plants (data not shown), indicating that water did not enter the pots. By contrast, soil water content increased quickly when plants were rewatered. Consistent with these data, Fig. 7 shows that the recovery of water potentials and hydraulic conductivity was much quicker in plants that were rewatered after the drought treatment than in plants that were transferred to the high-humidity environment without rewatering.

Water following a gradient in water potential from the epidermis towards the vascular tissue has to pass the bundle sheath (Fig. 1c). Radial cell walls of the bundle sheath are lignified, indicating that water molecules will cross cell membranes. AQPs are likely to play an important role in regulating the hydraulic resistance between vascular and photosynthetic tissues in conifer needles. Immunolocalization and *in situ* hybridization experiments confirmed the presence of AQPs in the endodermis-like bundle sheath of *P. glauca* needles. Although both PIP1 and PIP2 were detected in the bundle sheath, the PIP1 signal was stronger than the PIP2 signal in this cell layer (Fig. 2). This was also observed in a study on Norway spruce (*P. abies*) trees growing at

the timberline (Mayr *et al.*, 2014). In agreement with the immunolabeling results, *in situ* hybridization of *PgPIP1;1* antisense probes also showed a strong signal in the endodermis. We therefore suggest that PIP1s, and PgPIP1;1 in particular (Figs 4, 5e), play a critical role in mediating water flow through the endodermis.

PIP labeling was also detected in transfusion parenchyma and phloem cells. AQPs have been found previously in the leaf phloem of angiosperm species (Fraysse *et al.*, 2005; Hachez *et al.*, 2008), as well as in *P. abies* needles (Oliviusson *et al.*, 2001), consistent with a role for AQPs in phloem loading and unloading. In the context of foliar water uptake, radial water flow is probably directed towards vascular tissue, including phloem. Subsequently, water may move from needles to stems via the phloem. The unloading of water and solutes in stems may promote xylem refilling, as suggested for angiosperms (Nardini *et al.*, 2011). On the way from needles to stems, water may also move in the xylem; negative sap flow as a result of foliar absorption has been described in numerous studies (Burgess & Dawson, 2004; Nadezhdina *et al.*, 2010; Eller *et al.*, 2013; Goldsmith, 2013).

Figures 2 and 4 show the down-regulation of AQPs during drought. In leaves of *Arabidopsis*, PIP transcripts were also generally down-regulated in response to drought. The amount of protein was also reduced. Twenty-six hours after rehydration, the expression levels were back at the same level as in control plants (Alexandersson *et al.*, 2005). Consistent with these findings, Shatil-Cohen *et al.* (2011) proposed a role for bundle sheath cells as a stress signal-sensing 'control center' in leaves. According to their model, bundle sheath cells sense stress signals in the xylem sap (presumably abscisic acid) and respond by changing their hydraulic conductivity via the down-regulation of AQP activity. Our data are consistent with this idea. In addition, we show that the effect of drought on AQPs can be reversed by the exposure of leaves to high humidity.

The hypothetical chain of events summarized in Fig. 8 provides a theoretical framework that links foliar uptake with AQP function and embolism repair. Regardless of the mechanism, refilling in stem xylem occurred (Figs 6, 7), indicating that the uptake of water via needles was physiologically meaningful, and that this water moved from needles to stems. It remains to be tested whether needle water uptake occurs under natural conditions in the boreal forest. Conceivably, foliar water absorption could be beneficial during summer periods when the forest receives small quantities of rain that are not sufficient to penetrate the soil. Foliar water uptake may also occur on relatively warm days in late winter and early spring, whilst the ground is still frozen. Needles covered by melting snow may be able to absorb water and this could facilitate xylem refilling and offset winter desiccation effects, similar to that which has recently been shown for timberline trees in Austria (Mayr *et al.*, 2014).

The amount of xylem embolism during the drought treatment was relatively low, although stem water potentials of drought-stressed plants were close to −3 MPa (Fig. 6). *Picea glauca* stems exhibited no or minimal embolism at water potentials less negative than −2 MPa (Fig. 7). The shape of the vulnerability curve and the P50 value measured in this study agree with previously published values for *P. glauca.* Hacke & Jansen (2009) measured a P50 value of -4.3 ± 0.3 MPa ($\pm$ SE, $n = 6$), similar to the value of -4.6 ± 0.1 MPa ($\pm$ SE, $n = 6$) reported for sun-exposed trees by Schoonmaker *et al.* (2010).

Water potentials were not continuously monitored throughout the experiment, and so it is possible that Ψ_{Stem} increased to less negative values during the night. We therefore do not know whether refilling occurred at substantially negative water potentials, as reported by others (Sperry *et al.*, 1994; McCulloh *et al.*, 2011), or whether it was associated with a nocturnal increase in Ψ_{Stem} that was not captured. However, as pots were not watered, it is unlikely that Ψ_{Stem} reached values close to atmospheric pressure, which would be required for a purely physical dissolution of bubbles.

The present study provides the most comprehensive functional and phylogenetic analysis of spruce AQPs so far. The number of

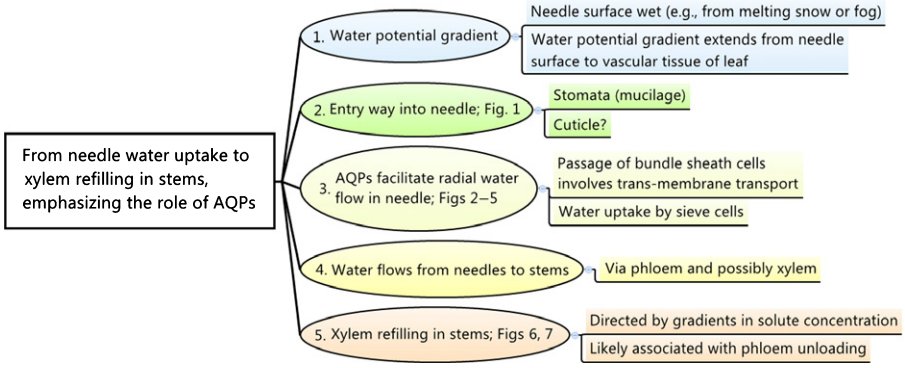

Fig. 8 Putative chain of events linking needle water uptake to xylem refilling in stems. Foliar water uptake may occur when a thin film of water has coalesced on the needle surface and the needle is experiencing a water deficit, that is, when the internal leaf tissue has a more negative water potential than the surrounding atmospheric boundary layer. Radial water movement inside the leaf also follows gradients in water potential and is directed from the epidermis towards vascular tissue. The passage of bundle sheath cells involves membrane transport, which is facilitated by aquaporins (AQPs; especially plasma membrane intrinsic proteins 1 (PIP1s)). Water uptake by sieve cells and other phloem cells may also be facilitated by aquaporins (especially PIP2s). Water then flows from needles to stems, where it contributes to embolism repair. Solutes and water are delivered from the phloem to embolized tracheids via rays. In this conceptual model, the direction of water flow is always consistent with gradients in water potential.

AQP genes in spruce is similar to the total number of MIPs reported for *Arabidopsis* (35, Johanson *et al.*, 2001) and maize (33, Chaumont *et al.*, 2001). In *Arabidopsis*, there are 13 PIPs (16 in *P. glauca*), 10 TIPs (nine in *P. glauca*), nine NIPs (four PgNIPs) and three SIPs (one PgSIP). In maize, 14 PIPs, 13 TIPs, five NIPs and three SIPs have been reported (Chaumont *et al.*, 2001). Hence, the distribution between the four major subfamilies is similar in these three species. However, both Arabidopsis and maize have more PIP1s than *P. glauca*. Consistent with this finding, Chaumont *et al.* (2001) noted that *ZmPIP1;3* and *ZmPIP1;4* are the result of a very recent gene duplication.

In conclusion, we report that needles of drought-stressed *P. glauca* plants absorb water when exposed to high RH. AQPs are present in the bundle sheath, in phloem cells and in transfusion parenchyma of needles. The up-regulation of AQP genes in high RH coincides with embolism repair in stem xylem. Our findings are consistent with the hypothesis that AQPs facilitate radial water movement from the needle epidermis towards the vascular tissue. Water may then move from needles towards stems via phloem and xylem (Fig. 8). Refilling in *P. glauca* is apparently not limited to xylem pressures near atmospheric values.

Acknowledgements

U.G.H. acknowledges funding from a Natural Sciences and Engineering Research Council (NSERC) Discovery grant, the Canada Foundation for Innovation and the Canada Research Chair program. The Saint-Modeste nursery, Quebec Ministry of Natural Resources provided plants for the experiment and technical assistance. We thank Amanda Schoonmaker for insightful comments on the potential role of foliar water uptake in the Canadian boreal forest.

References

Alba R, Fei Z, Payton P, Liu Y, Moore SL, Debbie P, Cohn J, D'Ascenzo M, Gordon JS, Rose JKC *et al.* 2004. ESTs, cDNA microarrays, and gene expression profiling: tools for dissecting plant physiology and development. *Plant Journal* **39**: 697–714.

Alexandersson E, Fraysse L, Sjovall-Larsen S, Gustavsson S, Fellert M, Karlsson M, Johanson U, Kjellbom P. 2005. Whole gene family expression and drought stress regulation of aquaporins. *Plant Molecular Biology* **59**: 469–484.

Almeida-Rodriguez AM, Hacke UG, Laur J. 2011. Influence of evaporative demand on aquaporin expression and root hydraulics in hybrid poplar. *Plant, Cell & Environment* **34**: 1318–1331.

Altschul SF, Madden TL, Schäffer AA, Zhang J, Zhang Z, Miller W, Lipman DJ. 1997. Gapped BLAST and PSI-BLAST: a new generation of protein database search programs. *Nucleic Acids Research* **25**: 3389–3402.

Arvidsson S, Kwasniewski M, Riano-Pachon D, Mueller-Roeber B. 2008. QuantPrime – a flexible tool for reliable high-throughput primer design for quantitative PCR. *BMC Bioinformatics* **9**: 465.

Begg JE, Turner NC. 1970. Water potential gradients in field tobacco. *Plant Physiology* **46**: 343–346.

Birol I, Raymond A, Jackman SD, Pleasance S, Coope R, Taylor GA, Saint Yuen MM, Keeling CI, Brand D, Vandervalk BP *et al.* 2013. Assembling the 20 Gb white spruce (*Picea glauca*) genome from whole-genome shotgun sequencing data. *Bioinformatics* **29**: 1492–1497.

Boucher JF, Munson AD, Bernier PY. 1995. Foliar absorption of dew influences shoot water potential and root-growth in *Pinus strobus* seedlings. *Tree Physiology* **15**: 819–823.

Braissant O, Wahli W. 1998. A simplified *in situ* hybridization protocol using non-radioactively labeled probes to detect abundant and rare mRNAs on tissue sections. *Biochemica* **1**: 10–16.

Breshears DD, McDowell NG, Goddard KL, Dayem KE, Martens SN, Meyer CW, Brown KM. 2008. Foliar absorption of intercepted rainfall improves woody plant water status most during drought. *Ecology* **89**: 41–47.

Burgess SSO, Dawson TE. 2004. The contribution of fog to the water relations of *Sequoia sempervirens* (D. Don): foliar uptake and prevention of dehydration. *Plant, Cell & Environment* **27**: 1023–1034.

Burkhardt J. 2010. Hygroscopic particles on leaves: nutrients or desiccants? *Ecological Monographs* **80**: 369–399.

Burkhardt J, Basi S, Pariyar S, Hunsche M. 2012. Stomatal penetration by aqueous solutions – an update involving leaf surface particles. *New Phytologist* **196**: 774–787.

Chang S, Puryear J, Cairney J. 1993. A simple and efficient method for isolating RNA from pine trees. *Plant Molecular Biology Reporter* **11**: 113–116.

Chaumont F, Barrieu F, Wojcik E, Chrispeels MJ, Jung R. 2001. Aquaporins constitute a large and highly divergent protein family in maize. *Plant Physiology* **125**: 1206–1215.

Chou K-C, Shen H-B. 2010. Plant-mPLoc: a top–down strategy to augment the power for predicting plant protein subcellular localization. *PLoS ONE* **5**: e11335.

Claros MG, von Heijne G. 1994. TopPred-II – an improved software for membrane-protein structure predictions. *Computer Applications in the Biosciences* **10**: 685–686.

Clifford SC, Arndt SK, Popp M, Jones HG. 2002. Mucilages and polysaccharides in Ziziphus species (Rhamnaceae): localization, composition and physiological roles during drought-stress. *Journal of Experimental Botany* **53**: 131–138.

Daniels MJ, Mirkov TE, Chrispeels MJ. 1994. The plasma membrane of *Arabidopsis thaliana* contains a mercury-insensitive aquaporin that is a homolog of the tonoplast water channel protein TIP. *Plant Physiology* **106**: 1325–1333.

Danielson J, Johanson U. 2008. Unexpected complexity of the aquaporin gene family in the moss *Physcomitrella patens*. *BMC Plant Biology* **8**: 45.

Eller CB, Lima AL, Oliveira RS. 2013. Foliar uptake of fog water and transport belowground alleviates drought effects in the cloud forest tree species, *Drimys brasiliensis* (Winteraceae). *New Phytologist* **199**: 151–162.

Fouquet R, Léon C, Ollat N, Barrieu F. 2008. Identification of grapevine aquaporins and expression analysis in developing berries. *Plant Cell Reports* **27**: 1541–1550.

Fraysse LC, Wells B, McCann MC, Kjellbom P. 2005. Specific plasma membrane aquaporins of the PIP1 subfamily are expressed in sieve elements and guard cells. *Biology of the Cell* **97**: 519–534.

Goldsmith GR. 2013. Changing directions: the atmosphere–plant–soil continuum. *New Phytologist* **199**: 4–6.

Goldsmith GR, Matzke NJ, Dawson TE. 2013. The incidence and implications of clouds for cloud forest plant water relations. *Ecology Letters* **16**: 307–314.

Gomes D, Agasse A, Thiébaud P, Delrot S, Gerós H, Chaumont F. 2009. Aquaporins are multifunctional water and solute transporters highly divergent in living organisms. *Biochimica et Biophysica Acta (BBA) – Biomembranes* **1788**: 1213–1228.

Gong HQ, Peng YB, Zou C, Wang DH, Xu ZH, Bai SN. 2006. A simple treatment to significantly increase signal specificity in immunohistochemistry. *Plant Molecular Biology Reporter* **24**: 93–101.

Gotsch SG, Asbjornsen H, Holwerda F, Goldsmith GR, Weintraub AE, Dawson TE. 2014. Foggy days and dry nights determine crown-level water balance in a seasonal tropical montane cloud forest. *Plant, Cell & Environment* **37**: 261–272.

Gupta AB, Sankararamakrishnan R. 2009. Genome-wide analysis of major intrinsic proteins in the tree plant *Populus trichocarpa*: characterization of XIP subfamily of aquaporins from evolutionary perspective. *BMC Plant Biology* **9**: 134.

Hachez C, Heinen RB, Draye X, Chaumont F. 2008. The expression pattern of plasma membrane aquaporins in maize leaf highlights their role in hydraulic regulation. *Plant Molecular Biology* **68**: 337–353.

Hacke UG, Jansen S. 2009. Embolism resistance of three boreal conifer species varies with pit structure. *New Phytologist* **182**: 675–686.

Hakman I, Oliviusson P. 2002. High expression of putative aquaporin genes in cells with transporting and nutritive functions during seed development in Norway spruce (*Picea abies*). *Journal of Experimental Botany* **53**: 639–649.

Heinen RB, Ye Q, Chaumont F. 2009. Role of aquaporins in leaf physiology. *Journal of Experimental Botany* **60**: 2971–2985.

Horton P, Park KJ, Obayashi T, Fujita N, Harada H, Adams-Collier CJ, Nakai K. 2007. WoLF PSORT: protein localization predictor. *Nucleic Acids Research* **35**: W585–W587.

Huang XQ, Madan A. 1999. CAP3: a DNA sequence assembly program. *Genome Research* **9**: 868–877.

Johanson U, Karlsson M, Johansson I, Gustavsson S, Sjovall S, Fraysse L, Weig AR, Kjellbom P. 2001. The complete set of genes encoding major intrinsic proteins in Arabidopsis provides a framework for a new nomenclature for major intrinsic proteins in plants. *Plant Physiology* **126**: 1358–1369.

Kammerloher W, Fischer U, Piechottka GP, Schäffner AR. 1994. Water channels in the plant plasma membrane cloned by immunoselection from a mammalian expression system. *Plant Journal* **6**: 187–199.

Karlgren A, Carlsson J, Gyllenstrand N, Lagercrantz U, Sundström JF. 2009. Non-radioactive *in situ* hybridization protocol applicable for Norway spruce and a range of plant species. *Journal of Visualized Experiments* **26**: 1205.

Katz C, Oren R, Schulze ED, Milburn JA. 1989. Uptake of water and solutes through twigs of *Picea abies* (L.) Karst. *Trees* **3**: 33–37.

Laur J, Hacke UG. 2013. Transpirational demand affects aquaporin expression in poplar roots. *Journal of Experimental Botany* **64**: 2283–2293.

Liesche J, Martens HJ, Schulz A. 2011. Symplasmic transport and phloem loading in gymnosperm leaves. *Protoplasma* **248**: 181–190.

Limm EB, Simonin KA, Bothman AG, Dawson TE. 2009. Foliar water uptake: a common water acquisition strategy for plants of the redwood forest. *Oecologia* **161**: 449–459.

Maurel C, Verdoucq L, Luu DT, Santoni V. 2008. Plant aquaporins: membrane channels with multiple integrated functions. *Annual Review of Plant Biology* **59**: 595–624.

Mayr S, Schmid P, Laur J, Rosner S, Charra-Vaskou K, Daemon B, Hacke UG. 2014. Uptake of water via branches helps timberline conifers refill embolized xylem in late winter. *Plant Physiology* **164**: 114.

McCulloh KA, Johnson DM, Meinzer FC, Lachenbruch B. 2011. An annual pattern of native embolism in upper branches of four tall conifer species. *American Journal of Botany* **98**: 1007–1015.

Nadezhdina N, David TS, David JS, Ferreira MI, Dohnal M, Tesař M, Gartner K, Leitgeb E, Nadezhdin V, Cermak J *et al.* 2010. Trees never rest: the multiple facets of hydraulic redistribution. *Ecohydrology* **3**: 431–444.

Nardini A, Lo Gullo MA, Salleo S. 2011. Refilling embolized xylem conduits: is it a matter of phloem unloading? *Plant Science* **180**: 604–611.

Néron B, Ménager H, Maufrais C, Joly N, Maupetit J, Letort S, Carrere S, Tuffery P, Letondal C. 2009. Mobyle: a new full web bioinformatics framework. *Bioinformatics* **25**: 3005–3011.

North GB, Lynch FH, Maharaj FDR, Phillips CA, Woodside WT. 2013. Leaf hydraulic conductance for a tank bromeliad: axial and radial pathways for moving and conserving water. *Frontiers in Plant Science* **4**: 78.

Nystedt B, Street NR, Wetterbom A, Zuccolo A, Lin YC, Scofield DG, Vezzi F, Delhomme N, Giacomello S, Alexeyenko A *et al.* 2013. The Norway spruce genome sequence and conifer genome evolution. *Nature* **497**: 579–584.

Ohrui T, Nobira H, Sakata Y, Taji T, Yamamoto C, Nishida K, Yamakawa T, Sasuga Y, Yaguchi Y, Takenaga H *et al.* 2007. Foliar trichome- and aquaporin-aided water uptake in a drought-resistant epiphyte *Tillandsia ionantha* Planchon. *Planta* **227**: 47–56.

Oliveira RS, Dawson TE, Burgess SSO. 2005. Evidence for direct water absorption by the shoot of the desiccation-tolerant plant Vellozia flavicans in the savannas of central Brazil. *Journal of Tropical Ecology* **21**: 585–588.

Oliviusson P, Salaj J, Hakman I. 2001. Expression pattern of transcripts encoding water channel-like proteins in Norway spruce (*Picea abies*). *Plant Molecular Biology* **46**: 289–299.

Pavy N, Boyle B, Nelson C, Paule C, Giguere I, Caron S, Parsons LS, Dallaire N, Bedon F, Berube H *et al.* 2008. Identification of conserved core xylem gene sets: conifer cDNA microarray development, transcript profiling and computational analyses. *New Phytologist* **180**: 766–786.

Plavcová L, Hacke UG. 2012. Phenotypic and developmental plasticity of xylem in hybrid poplar saplings subjected to experimental drought, nitrogen fertilization, and shading. *Journal of Experimental Botany* **63**: 6481–6491.

Rice P, Bleasby A, Ison J, Uludag M. 2000. EMBOSS: the European Molecular Biology Open Software Suite. *Trends in Genetics* **16**: 276–277.

Rigault P, Boyle B, Lepage P, Cooke JEK, Bousquet J, MacKay JJ. 2011. A white spruce gene catalog for conifer genome analyses. *Plant Physiology* **157**: 14–28.

Romualdi C, Bortoluzzi S, D'Alessi F, Danieli GA. 2003. IDEG6: a web tool for detection of differentially expressed genes in multiple tag sampling experiments. *Physiological Genomics* **12**: 159–162.

Rutledge RG, Stewart D. 2010. Assessing the performance capabilities of LRE-based assays for absolute quantitative real-time PCR. *PLoS ONE* **5**: e9731.

Sakurai-Ishikawa J, Murai-Hatano M, Hayashi H, Ahamed A, Fukushi K, Matsumoto T, Kitagawa Y. 2011. Transpiration from shoots triggers diurnal changes in root aquaporin expression. *Plant, Cell & Environment* **34**: 1150–1163.

Sauter J, Dörr I, Kollmann R. 1976. The ultrastructure of Strasburger cells (= albuminous cells) in the secondary phloem of *Pinus nigra* var. *austriaca* (Hoess) Badoux. *Protoplasma* **88**: 31–49.

Schoonmaker AL, Hacke UG, Landhausser SM, Lieffers VJ, Tyree MT. 2010. Hydraulic acclimation to shading in boreal conifers of varying shade tolerance. *Plant. Cell & Environment* **33**: 382–393.

Shatil-Cohen A, Attia Z, Moshelion M. 2011. Bundle-sheath cell regulation of xylem-mesophyll water transport via aquaporins under drought stress: a target of xylem-borne ABA? *Plant Journal* **67**: 72–80.

Sievers F, Wilm A, Dineen D, Gibson TJ, Karplus K, Li WZ, Lopez R, McWilliam H, Remmert M, Soding J *et al.* 2011. Fast, scalable generation of high-quality protein multiple sequence alignments using Clustal Omega. *Molecular Systems Biology* **7**: 539.

Simonin KA, Santiago LS, Dawson TE. 2009. Fog interception by *Sequoia sempervirens* (D. Don) crowns decouples physiology from soil water deficit. *Plant, Cell & Environment* **32**: 882–892.

Sparks JP, Campbell GS, Black RA. 2001. Water content, hydraulic conductivity, and ice formation in winter stems of *Pinus contorta*: a TDR case study. *Oecologia* **127**: 468–475.

Sperry JS, Donnelly JR, Tyree MT. 1988. A method for measuring hydraulic conductivity and embolism in xylem. *Plant, Cell & Environment* **11**: 35–40.

Sperry JS, Nichols KL, Sullivan JEM, Eastlack SE. 1994. Xylem embolism in ring-porous, diffuse-porous, and coniferous trees of northern Utah and interior Alaska. *Ecology* **75**: 1736–1752.

Thompson JD, Plewniak F, Ripp R, Thierry JC, Poch O. 2001. Towards a reliable objective function for multiple sequence alignments. *Journal of Molecular Biology* **314**: 937–951.

Vandeleur RK, Mayo G, Shelden MC, Gilliham M, Kaiser BN, Tyerman SD. 2009. The role of plasma membrane intrinsic protein aquaporins in water transport through roots: diurnal and drought stress responses reveal different strategies between isohydric and anisohydric cultivars of grapevine. *Plant Physiology* **149**: 445–460.

Supporting Information

Additional supporting information may be found in the online version of this article.

Fig. S1 Protein sequence alignment of *Picea glauca* major intrinsic proteins (MIPs).

Fig. S2 Neighbor-joining phylogeny of *Picea glauca* major intrinsic proteins (MIPs).

Fig. S3 Unweighted pair group method with arithmetic average (UPGMA) phylogeny of *Picea glauca* major intrinsic proteins (MIPs).

Fig. S4 Amino acid multiple sequence alignment of the N-terminal region of *Arabidopsis thaliana* AtPIP1;3 and the *Picea glauca* PgPIP1s and of the highly conserved 10 amino acids of the C-terminal region of PIP2s.

Table S1 Gene names, cDNA clone accession numbers, GenBank accession numbers, *Picea glauca* genome accession numbers and *P. abies* homolog genome accession numbers

Table S2 Primer sequences used for the gene expression study

Notes S1 Phylogenetic datasets.

Please note: Wiley Blackwell are not responsible for the content or functionality of any supporting information supplied by the authors. Any queries (other than missing material) should be directed to the *New Phytologist* Central Office.